Quenching a swarm: Effect of light exposure on suppression of collective motility in swarming *Serratia marcescens*

Alison E. Patteson[1,‡], Paulo E. Arratia[2] and Arvind Gopinath[3,‡]
[1]*Department of Physics, Syracuse University, Syracuse, NY.*
[2]*Department of Mechanical Engineering & Applied Mechanics, University of Pennsylvania, Philadelphia, PA 19104.*
[3]*Department of Bioengineering, University of California Merced, CA 95340.*
[‡]*aepattes@syr.edu, agopinath@ucmerced.edu*

Swarming colonies of the light sensitive bacteria *Serratia marcescens* grown on agar exhibit robust, fluctuating, collective flows that include vortices, jets and sinuous streamers spanning multiple bacterial lengths. Here, we study the effects of light, with a substantial ultra-violet component, on these collective flows. We expose regions of the swarm to light of different intensities and examine the accompanying changes in collective motility during exposure as well as immediately after cessation of exposure. For small exposure times and at low intensities, we find that collective mobility is negligibly affected. Increasing exposure times or intensity to higher values temporarily suppresses collective mobility. When the light is turned off, bacteria regain motility at the single cell level and eventually reestablish large scale flows. Thus with sub-optimal levels of light exposure, bacteria maintain a high chance of regaining collective motility. For long exposure times or high intensities, exposed bacteria are paralyzed and slow down, in the process forming jammed domains. The rate of formation of this jammed region and its initial dissolution rate upon ceasing exposure both strongly depend on duration of exposure. We hypothesize that this results from bacteria forming aligned domains as they slow down; erosion then involves dislodging bacteria from caged configurations. Our results complement studies on the effects of light on free-swimming bacteria and provide a foundation for studies on light-driven flow patterning in bacterial swarms.

I. INTRODUCTION

Swarming motility is a flagella driven form of bacterial surface migration that allows for rapid colonization of environments [1–8]. Widespread in many species of both Gram-positive and Gram-negative bacteria [3, 8], swarming is usually observed when free-swimming (planktonic) bacteria grown in fluids are subsequently transferred to soft wet agar gels [5]. The transfer triggers a change in phenotype; individual cells become significantly elongated and the number of flagella increases to 10–100 [1, 7]. At high enough densities beyond a critical value, the colony develops complex, long-range intermittent collective flow features that involving multiple bacteria traveling in rafts or flock-like clusters. The velocity fields are most prominent and intense near the edge of the expanding colony with the intensity decreasing with distance from the edge [2, 4, 5, 9]. Recent studies [10–12] demonstrate that swarming confers multiple benefits including enhanced colonization rates and elevated resistance to antibiotics when compared to other forms of bacterial motility. Swarming is also found to be co-regulated with virulence, and is thus implicated in infectiousness and fitness of pathogenic bacterial species [3, 7].

A significant challenge in understanding swarming motility is uncovering the relationship between the onset of collective motion and motility at the single cell level. Healthy bacterial cells sense spatiotemporally distributed cues, continuously process these inputs and transduce them to variations in motility and responses ([1, 4, 9, 13] and references therein). For instance, free-swimming bacteria respond to stimuli by modulating and controlling the molecular motors underlying flagellar motion [14–20]. Intense light with wavelengths in the range 290-530 nm encompassing the ultraviolet (UV) range is known to trigger changes in the motility of planktonic chemotactic bacteria [21–23]. For instance, changes in motility of *Escherichia coli* and *Streptococcus* arise from controlled variations in the tumble frequency, a behavior that requires requires the chemotaxis signal protein CheY [22, 24]. Prolonged exposure to high-intensity light results in progressively slow swimming with paralysis eventually occurring [21, 22] due to irreversible motor damage. It is however still unclear how swarming motility is affected by light-induced damage at cellular scales cells. Similar questions arise from studies on the chemotactic bacteria where modulation in the functioning of the MotA - MotB pair and FliG comprising the rotary motor complex in bacterial flagella is observed during chemotaxis. At the organismal scale, the net result is change in the trajectory - specifically, tumble length and turning frequency - that directs them towards nutrients and away from toxins [16, 19].

From a medical perspective, light treatment employing UV-A,B,C radiation is emerging as an attractive alternative to classical antibiotic treatment of pathogenic bacteria with exposure known to inhibit cell growth and induce gene damage [25], in marine organisms (alphaprotobacteria and bacterioplankton, [26]), airborne bacteria [27], as well in bacterial biofilms [28, 29]. Irradiation of surfaces using blue light and phototherapy that activates endogenous or exogenous photosensitizers [13, 30, 31] has

been shown to sterilize and disinfect bacteria laden surfaces. Swarming bacteria are susceptible to light in the presence of photosensitizer [13, 32] which disrupts the swarm motility by releasing reactive oxygen species (similar to other photosensitizing dyes). The effect of light on *Bacillus subtilis* [32] in the presence of photosensitizer reveals that as the bacterial cells become sluggish, the tendency to form flocks and large packs reduces and instead smaller clusters are observed. The overall reduction in cluster size and a less ordered motion within individual clusters gives rise to decreased correlation lengths with swarming eventually reverting to random motion in the presence of photodynamic effects. During exposure, the collective swarm velocity decays, a feature that can be recovered after exposure. Intense light is also known to promote wound healing [31, 33] with visible light recently approved to treat bacterial infections such as acne [34].

Given these promising studies and the timeliness of light treatments, understanding the connection between motility, infectiousness and light exposure is particularly important. In this article, we report on the effects of high intensity wide-spectrum light with a significant UV component on the swarming dynamics of *Serratia marcesens*. In collectively-moving swarms, individual cells are influenced by steric and hydrodynamic interactions with their neighbors [4–6, 35, 36]. These interactions result in macroscopic velocity speeds being different from the self-propulsion speed and furthermore yield complex features such as fluctuating regions of high vorticity. We start with unexposed swarming bacterial film exhibiting these complex features, expose localized regions of the swarm to wide-spectrum light and systematically identify exposure times and light intensities that *quench* the active swarm and rendering bacteria immotile. This may happen in either reversible or irreversible manner. We show that in addition to the direct effects of light such as reduced speed, there are secondary effects, including the creation of dense strongly jammed domains of immobile cells as the results of sustained exposure. These dense immobile domains hinder the penetration of unexposed bacteria into the region, thereby reducing total damage to bacteria in the colony. Post-exposure, swarming cells propagate into and populate the previously passive domain, dislodging and convecting immobile bacteria away. The dissolution process depends on the strength of the light exposure: bacteria exposed to sufficiently low light intensities recover their motility and erode the passive domain from within. Finally, we explore the growth and dissolution of the quenched domain and relate it to the duration of exposure and light intensity.

II. EXPERIMENTAL METHODS

Swarms of *Serratia marcesens* (strain ATCC 274, Manassas, VA) were grown on agar substrates, prepared by dissolving 1 wt% Bacto Tryptone, 0.5 wt% yeast extract, 0.5 wt% NaCl , and 0.6 wt% Bacto Agar in deionized water. Melted agar was poured into petri dishes, adding 2 wt% of glucose solution (25 wt%). *Serratia* were then inoculated on solidified agar plates and incubated at 34°C. Colonies formed at the inoculation sites and grew outward on the agar substrate from the inoculation site.

Swarms were studied and imaged 12-16 hours after inoculation. The bacteria were imaged with the free surface facing down with an inverted Nikon microscope Eclipse Ti-U using either a Nikon 10x (NA = 0.3) or 20x (NA = 0.45) objective. Images were gathered at either 30 frames per seconds with a Sony XCD-SX90 camera or at 60 frames per second with a Photron Fastcam SA1.1 camera. We used videos of the swarm and PIVLab software [37] to extract the velocity fields of the bacteria with particle image velocimetry (PIV) techniques. Particle image velocimetry determines velocity fields by calculating local spatial-correlations between successive images. Here, the images are of bacteria (either active or passive) such that PIV yields the bacterial velocity fields directly and not the velocity field of the ambient fluid.

To expose the bacteria to high intensity light, we use a wide spectrum mercury vapor lamp and standard microscope optics to focus the light on the swarm. We investigated the swarm's response as a function of exposure time and light intensities. The light intensity at the sample I_0 was varied by using neutral light density filters to reduce the unfiltered light intensity from the mercury lamp [38]. The intensity I_0 depends on the objective: using a spectrophotometer (Thorlabs, PM100D), we measured the intensity $I_0 = 980$ mW/cm^2 (at 535 nm) for the 10x objective and $I_0 = 3100$ mW/cm^2 (also at 535 nm) for the 20x objective.

III. RESULTS AND DISCUSSION

A. Phase-space for collective motility

Figure 1 shows the expanding edge of the colony, a region of which (white region exposed using an octagonal aperture) is exposed to high-intensity light from a mercury vapor lamp [38]. The swarm is expanding from left to right; the colony edge is indicated as the white edge in Figure 1. Bacteria swim in a thin layer above the agar substrate (inset, Figure 1). The thickness of the swarm varies with distance from the leading edge: studies on *E. coli* [39] showed that cells form a monolayer in the leading 30 μm of the colony, beyond which cells could form multi-layered regions. Overlaid on the image in Fig. 1 are bacterial velocity fields gathered from PIV; the image is taken after 80 seconds of exposure. Outside of the exposed region, the velocity field exhibits long-range collective flows. The unexposed bacteria move fastest approximately 100-400 μm from the colony edge (maximum speeds $\sim$80 μm/s, average speed $\sim$30 μm/s). In contrast, inside the exposed region, the bacteria are seen to move negligibly. We find that as swarming bacteria are exposed to light, they slow down and are eventually

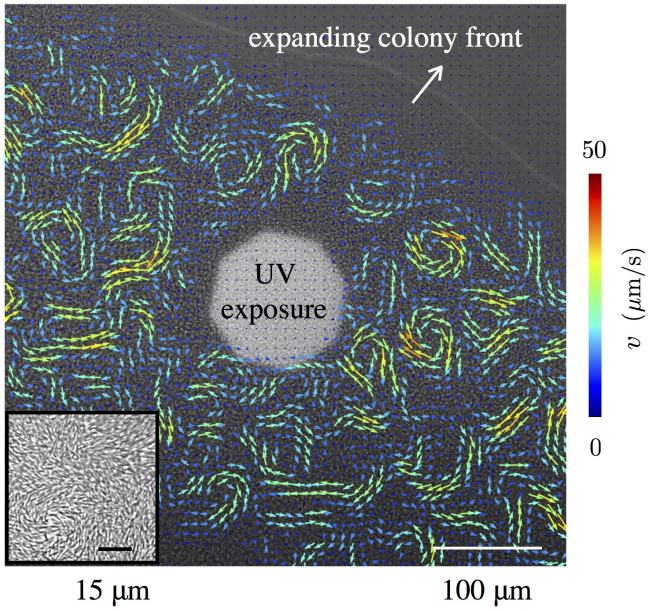

FIG. 1. Snapshot of a *Serratia marcescens* colony on an agar substrate, during exposure to high-intensity light from a mercury lamp source; PIV derived velocity fields are overlaid in color. Swarming motion is pronounced approximately 50 microns from the expanding colony front. The inset shows pre-exposure bacterial alignment and density 150 μm from the colony front.

trapped within the exposed region. This is seen in SI-Movie-1: small particles that serve as tracers slow down and eventually stop moving as they are trapped amongst the passive bacteria. The interphase boundary between the unexposed (passive) domain and the unexposed (active) part of the swarm features strong vortices, jets, and streamers, extending up to just a few microns away from the boundary of the exposed domain.

The quenching (passivation) of collective mobility of the initially active bacteria is not immediate and can be reversible depending on the intensity of light. In the experiment corresponding to Fig. 1, the exposed bacteria remain passive even after the wide-spectrum mercury lamp is switched off. In the absence of the light, the passive phase does not retain its shape or size; it is unstable and erodes as active swarming bacteria penetrate the passive domain and convect passive bacteria away. Based on these observations, we explore two features of the response to high intensity light: (i) the reversible versus irreversible nature of the bacterial response and (ii) the effects of exposure time and light intensities on the passive domain growth rate during exposure and dissolution rate post-exposure.

Figure 2 illustrates three different types of bacterial response to light for varying exposure times and intensities. We classify the response types based on the time-dependent velocity fields of the swarm: exposed cells either (i) remain moving, (ii) transiently stop moving, or (iii) permanently stop moving. To quantify the response, the phase behavior was mapped onto a phase diagram with exposure time τ and light intensity I as variables. For sufficiently small exposure times ($\tau \sim 20-40$ s) and intensities ($I < 220$ mW, at 535 nm), exposed cells remain always active. Conversely, for large exposure times ($\tau > 60$ s) and sufficiently high intensities ($I > 220$mW, at 535 nm), the bacteria are permanently passive (over the duration of the experiment). As shown in Fig. 2(a), between these two phases lies the temporarily passive, reversible case. We note that this intermediate case is not easily explained by assuming that exposure corresponding to a critical value of the net power determines the phase. A possible cause for this is that active swarming bacteria swim in and out of the exposed region.

The differences between the three motility regimes are highlighted in Fig. 2(b) and (c); these show PIV-derived velocity fields taken 10 seconds past exposure (Fig 2b) and the average bacterial speed $\langle v_c \rangle$ - in the exposed region - over time (Fig 2c). Here, $\langle v_c \rangle$ is the average speed of the velocity fields in a 22×22 μm^2 area, located at the center of the exposed region. In case (i), exposed cells remain motile and continue to exhibit long-range collective motions; the speed decreases but does not fully reach zero during exposure. The speed recovers to pre-exposure levels approximately 5 seconds after exposure. In case (ii), bacteria stop moving during exposure, yet spontaneously start moving again $\sim$ 1-10 s after the light is switched off. The cell speed $\langle v_c \rangle$ takes longer to recovers to pre-exposure levels than case (i), and the recovery occurs heterogeneously with cells moving within the temporally-quiescent region (Fig. 2(b)-ii). This process resembles a frozen domain that melts heterogeneously from various locations. In case (iii), cells stop moving during exposure and do not regain their motility afterward for the whole duration of the experiment (20-300 s). Unlike case (ii), cells in the exposed region here do not spontaneously regain their motility (Fig. 2(b)-iii). We find that, in this case, the passive domain evolves solely due to its interaction with the active swarm at its boundary. The active swarm convects passive bacteria away from the boundary and the passive phase is dismantled entirely; the speed $\langle v_c \rangle$ eventually increases (Fig. 2(c)-iii) as the swarm recaptures the quenched area. The regimes in the phase-plot (Figure 2(a)) can be rationalized by assuming the existence of a lower threshold for the intensity $I_{\min}$ below which bacteria are not affected. The response to light involves changes to the motor complex and possibly involves a cascade of biochemical events. However, in terms of interpreting Figure 2, these biochemical time-scales may be treated in an approximate phenomenological way by using a lumped time approximation. Specifically, we invoke an intrinsic time scale τ_* that determines the internal organismal response to light resulting in either temporary ($\tau_* = \tau_{\rm temp}$) or permanent ($\tau_* = \tau_{\rm perm}$) passivation. The curves that separate the

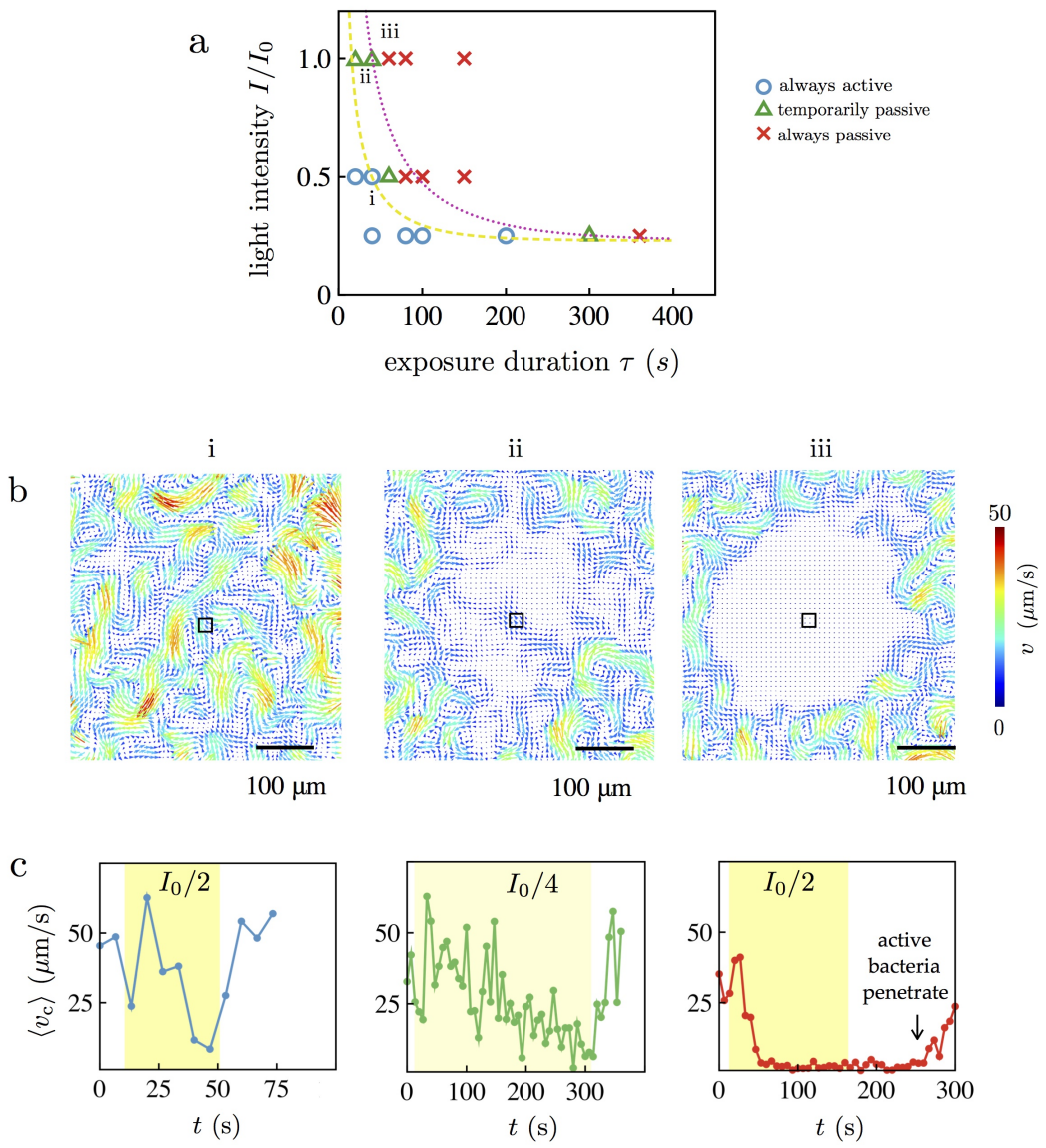

FIG. 2. **(a)** Changes in collective flows (relative to the unexposed state) in swarming *Serratia marcescens* depend strongly on intensity and duration of light exposure. Using a wide spectrum mercury lamp (bare intensity $I_0 = 980$ mW/cm^2 at 535 nm) with filters to selectively expose regions of the swarm, and from subsequent PIV analysis of bacterial velocities, the response can be classified into one of three types - (i) always active, (ii) temporarily passive, and (iii) always passive. The yellow (dashed) and pink (dotted) curves are phase boundaries predicted by equation 1. **(b)** Velocity fields taken 10 s post exposure are shown for each phase. Colors reflect speed with the arrows denoting polar orientation. Collective motility of temporarily immobile bacteria is recovered in approximately 15 seconds past exposure. **(c)** We plot the average speed of the swarm in the central region, highlighted by the box in **(b)** for times encompassing pre-exposure, exposure (yellow band), and post-exposure. Pre-exposure, the average swarm speed fluctuates between 25-50 μm/s. For case (i), the bacteria briefly slow down during exposure, but recover in 6 s. In (ii), the swarm speed approaches zero during exposure and recovers in 12s. In (iii), the collective swarm speed drops to and remains zero.

different responses in Figure 2(a) may then be fit by

$$\frac{I(\tau)}{I_0} = A \exp(-\frac{\tau}{\tau_*})\Big(1 + \frac{\tau_*}{\tau}\Big) + I_{\min} \qquad (1)$$

where the constants $(A, I_{\min}, \tau_{\text{temp}})$ are $(0.2, 0.23, 62)$ for the yellow (dashed) curve and $(A, I_{\min}, \tau_{\text{perm}})$ are $(0.33, 0.23, 100)$ for the pink (dotted) curve. As expected we note that $\tau_{\text{temp}} < \tau_{\text{perm}}$. The variation in A reflects the fact that our experiments do not probe the short time, $\tau \to 0$, high intensity exposure $I/I_0 \gg 1$ limit.

Similar responses have been observed earlier in studies on *E. coli* and *S. typhimurium* [21]. Specifically, prolonged exposure to unfiltered light in both bacterial species resulted in constant tumbling, then smooth swimming, and eventually paralysis. *S. typhimurium* was

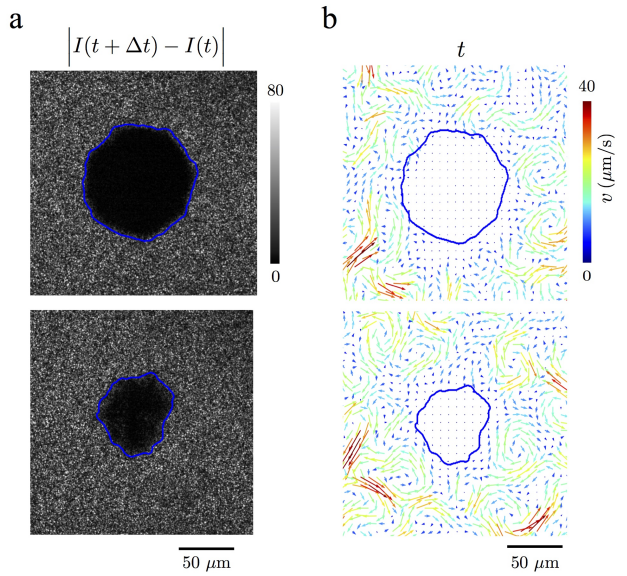

FIG. 3. We use intensity fluctuations to distinguish between the quenched (passive) and motile (active) regions. (a) We calculate an intensity fluctuation map $|I(t+\Delta t) - I(t)|$, with $\Delta t = 0.1$ seconds. Intensity fluctuations are low (black) in the regions where the swarm is not moving. The map when thresholded allows us to identify the boundary position (blue contours). The passive phase shrinks as time goes by as shown at $t = 1$ sec (top) and $t = 40$ sec (bottom) post-exposure (Exposure duration $\tau = 80$ sec, Intensity is $I = 3$ W/cm^2 measured at wavelength 535 nm). (b) PIV derived bacteria velocity fields confirm the boundary location obtained from the intensity fluctuation maps. A mathematically defined diffuse boundary may be obtained from phase field profiles [40] using order parameters [41]; here however, we use simple thresholding.

found to responds instantaneously to exposure with recovery of normal motility in 2 s or less upon cessation of exposure provided the duration of exposure was less than 5s. Similarly, *E. coli* recovered normal motility in 1 to 10 s after cessation of exposure. Sustained exposure that ultimately results in paralysis was however found to be irreversible (with no recovery of motility even after 15 minutes) for both species.

B. Thresholding yields extent of quenched domain

To determine the extent of the quenched (passive) domain, we use two methods, one based on image intensity fluctuations [42, 43] and the second based on PIV derived velocity fields and both involving a simple threshold criteria. The image intensity fluctuations are defined here as

$$|\Delta I(\mathbf{r}, t, \Delta t)| = |I(\mathbf{r}, t + \Delta t) - I(\mathbf{r}, t)|, \qquad (2)$$

where $I(\mathbf{r}, t)$ is the two-dimensional image intensity at pixel position $\mathbf{r}$ and Δt is the time step. We choose $\Delta t = 0.1$ sec, which corresponds to the time in which a swarming *Serratia* cell swimming at 50 μm/s moves roughly a body distance (5 μm). To reduce noise in the system (due to pixel resolution, short-range fluctuations, and background light fluctuations), we filter pixel-wise $|\Delta I(\mathbf{r}, t, \Delta t)|$ by smoothing over 3x3 μm^2 areas.

As shown in Fig. 3, the intensity fluctuations distinguish two domains, the immobile domain where values of $|\Delta I|$ are relatively small and the motile domain where $|\Delta I|$ are relatively large. We threshold $|\Delta I|$ to obtain a locus of points that defines the boundary of the active and passive phases. We checked that our results do not depend on the exact choice of Δt in the range 0.05 s $< \Delta t <$ 0.3 s. The locations of the active and passive domains, as well as their relative sizes such as area, match between the two methods, although the intensity fluctuations identifies smaller features of the boundary compared to the coarse-grained spatially-averaged bacterial velocity fields from PIV (Fig. 3(b)). Together, these metrics capture complimentary aspects of the swarm's motility: the intensity fluctuations are a scalar measure of density fluctuations and PIV yields vectorial velocity fields (i.e, the instantaneous polarity fields). Suitably thresholding the intensity fluctuations and/or PIV derived velocity fields, we can define a physically meaningful boundary that separates the quenched region from the swarm. This approach can be formalized in order to extract the location and width of the interface ([40, 41]); however for the results presented in this paper, it suffices to work with the magnitude of the fluctuations and the velocity fields.

C. Form and growth of the quenched region

We next analyze the role of the exposure time τ (that together with the intensity determines the total exposure) on the shape, size, and dissolution rate of the passive domain in the active swarm that ensues when the source of light is switched on and then switched off. These experiments, unless stated otherwise, were conduced at with intensity $I = 3100$ mW/cm^2 (at 535 nm); exposure times were varied from 10-300 seconds.

Exposure to light in our system is akin to a quench with activity *modified and thus in a sense removed* from our system. That is, exposure reduces the activity or energy in the system by removing the ability of bacteria to self-propel and thence initiate large scale collective motions. Furthermore, bacteria slow down while still diffusing thermally; thus they end up in tightly jammed clusters with distinct aligned domains (Figure 3(a)). It is thus of interest to examine the time-dependent velocity fields and the time-dependent growth of the passivated region.

We calculate a coarse-grained one-dimensional profile of the bacterial speed $\langle v(r, t)\rangle$, exploiting the symmetry

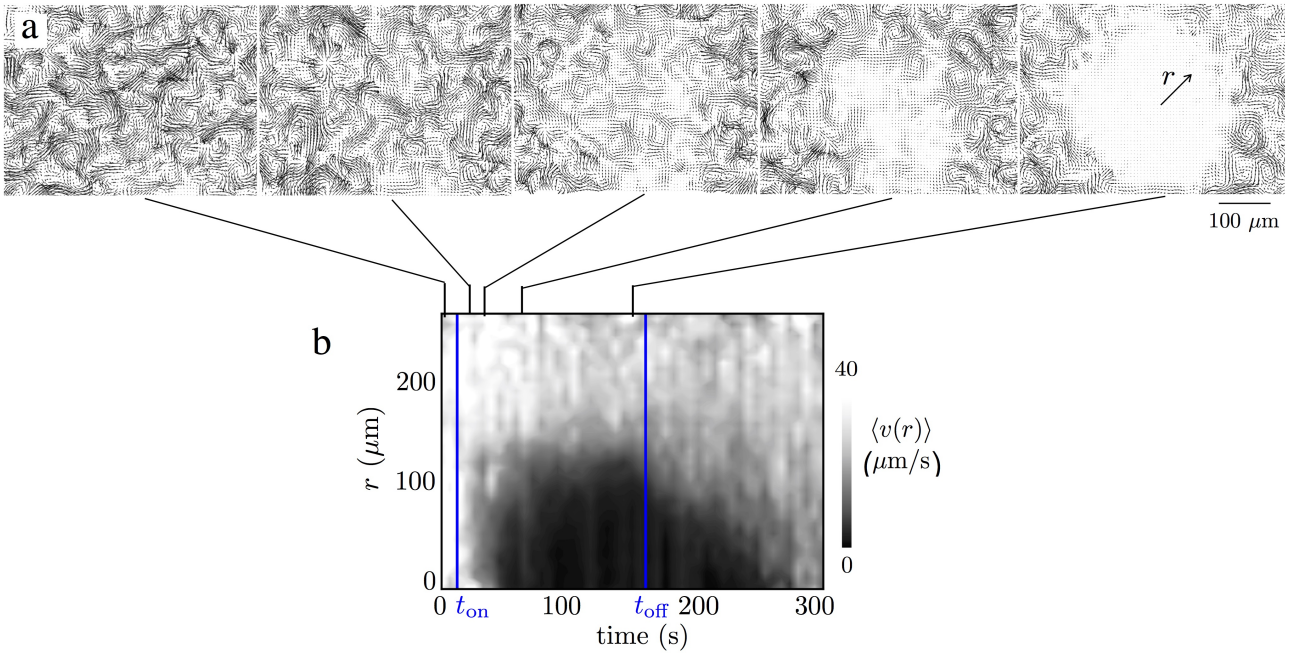

FIG. 4. (a) (Top) PIV derived bacterial velocity fields before and during light exposure. (Bottom) The azimuthally averaged velocity $\langle v(r)\rangle$ highlights the creation of an immobile quenched domain within the exposed region. When the light is switched off, the active bacteria from the unexposed regions penetrate into the quenched domain, eroding it away. The intensity I_0= 500 mW/cm^2. We note the brief lag after the light is switched on ($t_{\rm on}$), the gradual increase to a finite size as $t \to t_{\rm off}$ and the rapid erosion and mixing with the grey interphase region $t > t_{\rm off}$.

of the system and averaging the bacterial speed from PIV over the azimuthal angle. This yields a mean velocity field that is a function of the radial distance r from the center of the exposed region.dependence from the center of the exposed. Figure 4 shows a contour plot of $\langle v(r)\rangle$ over time t and corresponding snapshots of the two-dimensional velocity field. The passive domain appears in the contour plot (Fig. 4b) as the dark region where the bacterial speed is zero.

When the light source is turned on, the bacterial speed in the exposed region decreases in a non-uniform manner, diminishing the most in the center of the exposed region (Fig. 4a). The two dimensional velocity fields suggest that bacteria stop moving in multiple sub-domains, each of which continuously interact with active bacteria that are still moving. It takes approximately 50 seconds of exposure for a spatially-uniform passive domain to develop. This time value is likely dependent on bacterial diffusivity, time for going from the temporarily passive to fully immobile phase and the increasing jammed situation paralyzed bacteria experience. It is also at this state that local flocks can form in an aligned manner in order to accommodate the increasing jamming - thus forming a dense jammed quenched phase. After this initial lag time $t_{\rm lag}$, the size of the passive domain increases monotonically with time t during exposure increasing rapidly with a small momentum boundary layer at the edge. Fluctuations in r^* are due to variations in the heterogeneous, fluctuating velocity fields during exposure (Fig. 4a).

When the light is turned off, active bacteria penetrate the passive phase and convect passive bacteria away. The advancing swarm increases the average bacterial speed as it propagates radially inward, as seen in Fig. 4b. In approximately 100 seconds post exposure, the active swarm recaptures the exposed domain. We note that the boundary layer (fuzzy region) at the edge of the rapidly eroding quenched domain is larger than when the domain is being formed.

The effective size r^* of the passive domain (Fig. 5c) can be discerned by thresholding the values of $\langle v\rangle$. We select a threshold of 10 μm/s, which is much less than the average speed of the active region (40 μm/s) while large enough to average over small fluctuations. Adjusting for the lag time (Figure 5), we find that the radius of the quenched region $r*(t) \approx \sqrt{t-(t_{\rm lag}+t_{\rm on})}$ with $t_{\rm on}$ being the time when the light source is turned on (Fig. 5). Large variations in r^* are a consequence of asymmetric formation of the jammed domain. The square-root dependence is robust when the passive domain starts to form but is not as good a fit as the passive domain saturates to a radial extent slightly less than the size of the exposed region (120 μm).

Figures 6a and 6b provide insight into the size of the passive domains that form and their shapes as a function of the exposure times τ. To adjust the viewing window, the 60 μm aperture experiments are done with a 20x objective and the 120 μm aperture with a 10x objective, noting that the light intensity is higher for the

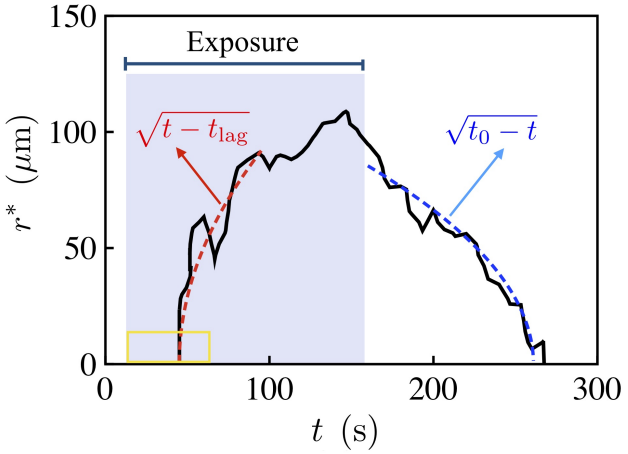

FIG. 5. Growth and dissolution of the quenched domain. The effective size of the quenched (passive) domain grows during exposure, stabilizes while illuminated and then erodes once the light is switched off. Selecting the contour of points corresponding to $\langle v \rangle = 10$ μm/s (evaluated from Fig. 4(b)) we calculate the instantaneous effective size r^* of the quenched region. When the light source is turned on at $t_{\rm on}$, r^* increases from zero only after an apparent lag time $t_{\rm lag} \approx 50$s. Lowering the threshold velocity yields a very noisy initial growth region but with an apparently shorter lag. The initial growth has a square root dependence with time (red dashed curve). Post-exposure, r^* follows a square root scaling as well (blue dashed curve). We observe deviations of around $5 - 10$ μm in these curves due to variations in the velocity field. The aperture size used here is 120 μm.

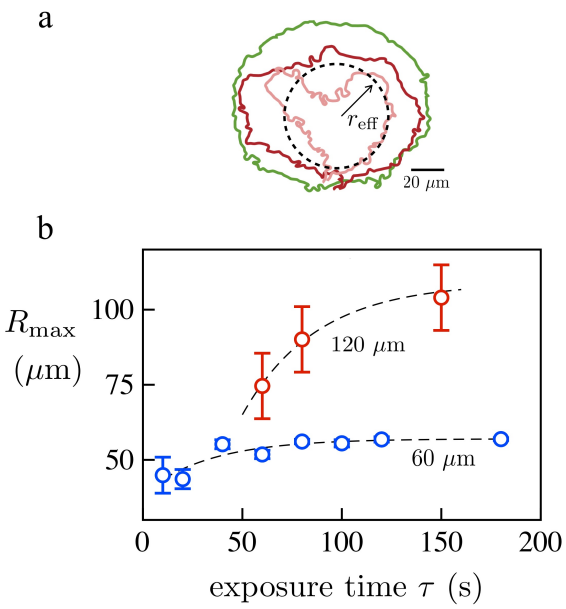

FIG. 6. (a) Typical interface positions $\mathbf{r}_{\rm I}$ of the passive region obtained from the locus of points $\phi(\mathbf{r}_{\rm I}, t = t_{\rm off})$ with $r_{\rm eff}$ indicated. The pink, red and green curves correspond to exposure times of 10, 20 and 100 seconds with the exposure occurring through an aperture of size 60 μm and 20x objective. (b) The maximum effective size of the passive phase $R_{\rm max}$ increases with exposure duration τ and asymptotes to a constant that is less than the aperture size.

60 μm aperture case at 20x. To quantify the mean and variance of the data, we plot the average from four experiments with corresponding to the standard deviation shown as error bars. We track the un-averaged boundary positions $\mathbf{r}_{\rm I}(t)$ from the image intensity fluctuations $|\Delta I|$ using Equation 2. We then estimate the effective size of the passive phase $r_{\rm eff}$ by calculating the radius of gyration of the boundary positions following

$$r_{\rm eff}(t) = \sqrt{\int_{\rm Passive} |\mathbf{r}_{\rm I} - \bar{\mathbf{r}}|^2 \, d\mathbf{r}} \qquad (3)$$

where $\bar{\mathbf{r}}$ is the center of mass at time t. The maximum size of the passive phase $R_{\rm max}$ equal to $r_{\rm eff}(t = t_{\rm off})$, when the size of the passive phase is seen to be greatest. Here the time at which exposure is terminated is $t_{\rm off}$.

From Figure 6a (aperture size 60 μm), it is clear that exposure times result in incompletely quenched and irregular, asymmetric domains. As the exposure time is increased, the domains become larger (eventually comparable to the aperture size) and more regular. The maximum intensity of light is at the center of the aperture and so the quenching starts there with the boundary propagating outward. The domain size $r_{\rm max}$ increases with τ and asymptotes to a constant that is slightly less than the aperture size (Fig. 6b); the asymptote is approximately 58 μm for the 60 μm aperture. For aperture size 120 μm, we find the limiting asymptote to be ≈ 169 μm. The data in Fig. 6b fits the functional form

$$r_{\rm max} = r_{\rm F} - b \exp\Big(-\tau/\tau_c\Big), \qquad (4)$$

with $r_{\rm F} = 57$ μm, $b = 18$ μm, and $\tau_c = 33.5$ s for the 60 μm aperture and $r_{\rm F} = 109$ μm, $b = 169$ μm, and $\tau_c = 37.3$ s for the 120 μm aperture.

We find that the size of the passive phase post-exposure as determined by the velocity maps (Fig 5) closely follows $r^* \sim \sqrt{t_0 - t}$; here t_0 is the time at which the passive phase completely disappears. Based on this observation, we then studied how $r_{\rm eff}$ decreases over time for various exposure durations (Figure 7a). Surprisingly, we find that the square-root scaling hold for small exposure times as well with t_0 as expected increasing with exposure time. At a qualitative level, and using the language of diffusive processes (in this case of the active momentum), this trend may be understood as resulting from the competing influences of effective active diffusivity, variations in the density and alignment of immobile bacteria in the passive phase. In our active, far-from equilibrium system, the passive domain is eroded by single bacteria-bacteria interactions (displacements originating from steric and self-propulsive mechanisms) as well as by collective highly non-equilibrium flow structures that

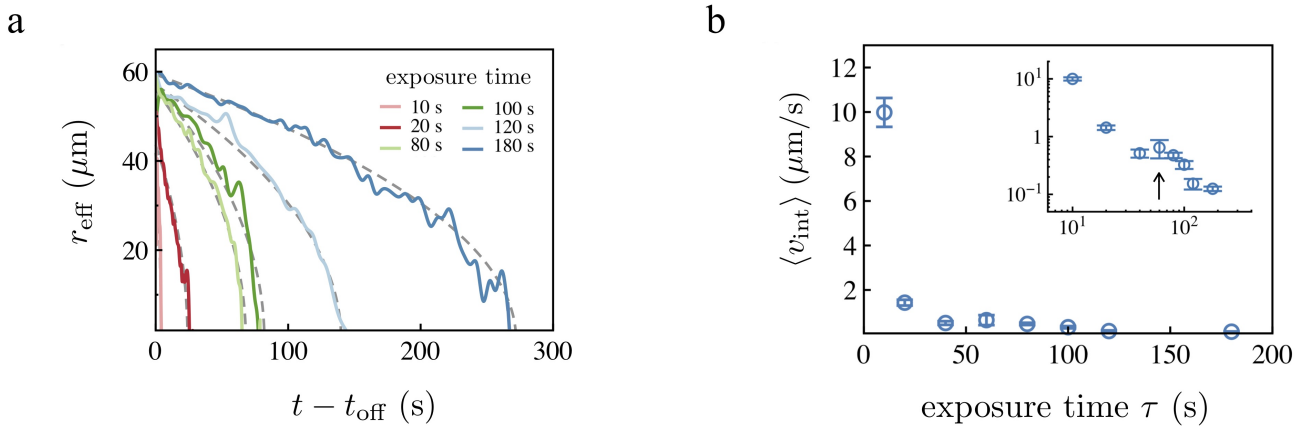

FIG. 7. (a) The effective extent of the quenched, passive domain decreases over time t at rates that depend on the exposure duration τ reflecting the influence of the alignment effects due to jamming as the bacteria are exposed to light. Longer exposure times prolong erosion by the active swarming bacteria, increasing the time it takes for the passive phase to disappear (at time t_0). For each τ, the effective size $r_{\rm eff}$ follows $r_{\rm eff} \approx \sqrt{t_0 - t}$ (grey dashed curves) with $t_0(\tau)$ being the time for complete dissolution. (b) The average initial dissolution velocity $\langle v_{\rm int} \rangle$ decreases significantly with τ. The trend may indicate non-monotonicity - given the size of the error bars, we are however unable to state this conclusively. Data is the average calculated from four experiments with standard deviation as error bars ($I \approx 3$ W/cm^2).

form near the surface. Understanding of this scaling requires a consideration of the coupling between interface shape, interface speed and interface flow fields [41].

Finally, we also measure the initial boundary dissolution speed by calculating $\langle v_{\rm int} \rangle = \big(r_{\rm eff}(t_{\rm off}) - r_{\rm eff}(t_{\rm off} + \Delta t)\big)/\Delta t$, where $\Delta t = 10$ seconds. We find that $\langle v_{\rm int} \rangle$ varies significantly with exposure time (Figure 7b), decreasing from 10 μm/s to 0.1 μm/s as τ increases from 10 to 300 seconds. The decrease in speed is not monotonic, rather we observe a peak (inset) that is not ascribable to experimental variations. Large exposure times are expected to yield different bacterial orientations in the passive region during the jamming and quenching process. It is also possible that variations in exposure time changes the cell motility in the active unexposed phase due to UV effects leaching into the active phase and hindering cell motility in the unexposed region. These effects may result in different physical micro-scale mechanisms that dominate the erosion just when exposure is stopped.

IV. CONCLUSIONS

The motion of dense bacterial suspensions or swarming bacterial can be impacted by light in two ways - 1) at the level of single organisms where UV can impact tumbling and therefore speed as well as diffusivity, and 2) at the collective level, where small regions of immobile bacteria can can both effectively blocking parts of space accessible to swarms as well as trap motile bacteria, thereby prevent them from escaping the light and eventually forming large quenched jammed domains.

We find that the *collective motility* of swarming *S*erratia marcescens displays a range of behaviors in response to UV light. At minimum exposure levels, swarms withstand the effects of light on their ability to move and maintain long-range collective motions. For sufficiently intense exposures, bacteria are rendered stationary by the UV light, an effect that is either reversible or irreversible, depending on the exposure level. The passive domain occurs for critical values of illumination power, requiring a minimum exposure time to appear. Longer exposure times prolongs the dissolution of the passive phase by the active swarming bacteria. Note that local weakly interacting, high aspect ratio passive polar rods can organize into highly ordered states [44] through flow, steric interactions or other weakly aligning interactions. The slowing of individual bacteria, disruption of their self-propulsion and the further orienting affects of local shearing motions by neighboring bacteria may allow similar mechanisms to operate here and result in the formation of strongly aligned and jammed phases. Erosion of these will involve dislodging bacteria from geometric cages and traps and require longer times and stronger flows.

Our results are relevant to the use of ultraviolet light to sterilize bacteria at densities high enough that they are not free-swimming. When exposed bacteria are rendered permanently immobile, jammed passive bacteria may act as a physical barrier and hinder the flux of unexposed bacteria; thus only a small fraction of the bacteria that are directly exposed are disinfected. Furthermore, evolution through mutation and selection in natural bacterial populations allow bacterial populations to differentiate genetically and phenotypically and better adapt to the damaging effects of light. Understanding this process requires the systematic study of light exposure on both free-swimming and collectively interacting bacteria. Bacteria that are able to recover may be genetic variants predisposed to UV resistance. Reestablishing collective

motility, and upon subsequent cell divisions, these cells may eventually result in emergence of resistant strains. It is important to study the effects of light on different swarming phenotypes, planktonic phenotypes, and other variants to understand the contribution of cell motility and active/passive particle interactions [45] on the survival of the swarm.

ACKNOWLEDGEMENTS

We would like to thank Ed Steager and Elizabeth Hunter for providing the cells and experimental assistance. AEP AND PEA acknowledge funds from NSF-DMR-1104705 and NSF-CBET-1437482. AEP was supported by an NSF Graduate Research Fellowship. AG acknowledges support through startup funds from the University of California, Merced.

[1] L Alberti and RM Harshey, J Bacteriol. 172(8), 4322 (1990).
[2] RM Harshey, Annu Rev Microbiol. 57, 249 (2003).
[3] N Verstraeten, Trends Microbiol. 16(10), 496 (2008).
[4] MF Copeland and DB Weibel, Soft Matter 5(6), 1174 (2009).
[5] NC Darnton, L Turner, S Rojevsky, and HC Berg, Biophys. J. 98(10), 2082 (2010).
[6] L Turner, R Zhang, NC Darnton and HC Berg, J Bacteriol. 192(13), 3259 (2010).
[7] DB Kearns, Nat Rev Microbiol. 8(9), 634 (2010).
[8] RM Harshey and JD Partridge, J Mol Biol. 427(23), 3683 (2015).
[9] EB Steager, C-B Kim and MJ Kim, Phys Fluids 20, 073601 (2008).
[10] MT Butler, Q Wang and RM Harshey, Proc Natl Acad Sci USA 107(8), 3776 (2010).
[11] D Roth *et al.*, Environ Microbiol. 15, 2532 (2013).
[12] S Lai, J Tremblay and E Deziel, Environ Microbiol. 11(1), 126 (2009).
[13] C Chen, S Liu, X-Q Shi, H Chate and Y Wu, Nature 542, 210 (2017).
[14] HC Berg and DA Brown, Nature 239, 500 (1972).
[15] JB Mitchell, Am Nat. 160, 727 (2002).
[16] HC Berg, *E. coli in Motion*, Springer (2008).
[17] J Adler, Science 153(3737), 708 (1966).
[18] GH Wadhams and JP Armitage, Nat Rev Mol Cell Biol. 5(12), 1024 (2004).
[19] HC Berg and RA Anderson, Nature 245, 380 (1973).
[20] AE Patteson, A Gopinath, M Goulian and PE Arratia, Scientific Reports 5, 15761 (2015).
[21] BL Taylor and DE Koshland Jr, J Bacteriol. 123(2), 557 (1975).
[22] S Wright *et al.*, J Bacteriol. 188(11), 3962 (2006).
[23] E Steager *et al.*, Appl Phys Lett. 90(26), 263901 (2007).
[24] MP Conley and HC Berg, J Bacteriol. 158(3), 832 (1984).
[25] http://medicalmate.gr/img/cms/UVC (2015)
[26] L Alonso-Saez, JM Gasol, T Lefort, J Hofer and R Sommaruga, Appl Environ Microbiol. 72(9), 5806 (2006).
[27] DG Sharp, J Bacteriol. 39(5), 535 (1940)
[28] M Ben Said, S Khefacha, L Maalej, I Daly and A Hassen African Journal of Microbiology Research 5(25), 4353 (2011).
[29] B Li and BE Logan, Colloids Surf B Biointerfaces 41(2-3), 153 (2005).
[30] CM Abana *et. al.*, Microbiologyopen. 6(4): e00466 (2017).
[31] T Dai, MS Vrahas, CK Murray and MR Hamblin, Expert Rev Anti Infect Ther. 10(2), 185 (2012).
[32] S Lu, W Bi, F Liu, X Wu, B Xing and EKL Yeow, Phys Rev Lett. 111, 208101 (2013).
[33] T Dai *et al.*, Antimicrob Agents Chemother. 57(3), 1238 (2013).
[34] S Pei, AC Inamadar, KA Adya and MM Tsoukas, Indian Dermatol Online J. 6, 145 (2015).
[35] S Bensity, E Ben-Jacob, G Ariel and A Be'er, Phys Rev Lett. 114, 018105 (2015).
[36] AE Patteson, A Gopinath and PE Arratia, Current Opinion in Colloid & Interface Science 21, 86 (2016).
[37] W Thielicke and E Stamhuis, J Open Research Software. 2(1), e30 (2014).
[38] http://zeiss-campus.magnet.fsu.edu/print/lightsources/mercuryarc-print.html
[39] Y Wu and HC Berg, Proc Nat Acad Sci USA 109(11), 4128 (2012).
[40] A Gopinath, RC Armstrong and RA Brown, J Cryst Growth 291 (1), 272 (2006).
[41] AE Patteson, A Gopinath and PE Arratia, (Submitted) (2018).
[42] R Cerbino and V Trappe, Phys Rev Lett. 100, 188102 (2008).
[43] LG Wilson *et. al.*, Phys Rev Lett. 106, 018101 (2011).
[44] A Gopinath, L Mahadevan and RC Armstrong, Phys Fluids 18, 028102 (2006).
[45] AE Patteson, A Gopinath, PK Purohit and PE Arratia, Soft Matter 12(8), 2365 (2016).